Proceedings of the ASME 2010 3rd Joint US-European Fluids Engineering Summer Meeting and 8th International Conference on Nanochannels, Microchannels, and Minichannels
FEDSM-ICNMM2010
August 1-5, 2010, Montreal, Canada

FEDSM-ICNMM2010-31257

CHARACTERIZATION AND OPTIMIZATION OF A THREE DIMENSIONAL T-TYPE MICROMIXER FOR CONVECTIVE MIXING ENHANCEMENT WITH REDUCED PRESSURE LOSS

Cesar A. Cortes-Quiroz*
Department of Mechanical Engineering
cesar.cortes@ucl.ac.uk

Alireza Azarbadegan
Department of Mechanical Engineering

Mehrdad Zangeneh
Department of Mechanical Engineering

University College London, Torrington Place, Roberts building 4th floor, London WC1E 7JE, UK

ABSTRACT

Numerical simulations and experiments are used to evaluate the flow and mixing characteristics of a proposed convective 3-D T-type micromixer. The study presents a parametric study and performance optimization of this micromixer based on the variation of its geometry.

To investigate the effect of design and operation parameters on the device performance, a systematic design and optimization methodology is applied; it combines Computational Fluid Dynamics (CFD) with an optimization strategy that integrates Design of Experiments (DOE), Surrogate modeling (SM) and Multi-Objective Genetic Algorithm (MOGA) techniques. The degree of mixing and the pressure loss in the mixing channel are the performance criteria to identify optimum designs at different Reynolds numbers (Re).

The convective flow generated in the 3-D T-type micromixer drastically enhances mixing at Re > 100 by making the two fluids to roll up along the mixing channel.

The resulting optimum designs are fabricated on polymethylmethacrylate (PMMA) by CNC micromachining. Experiments are carried out to visualize the streams of de-ionized water and aqueous fluorescein solution, by which the extent of mixing is determined, based on the standard deviation of fluorescein intensities on cross-section images.

This study applies a systematic procedure for evaluation and optimization of a proposed 3-D T-mixer which has a configuration of channels that promote convective mixing since the two fluids come into contact. The methodology applied can also be used to efficiently modify and customize current micromixers.

1 INTRODUCTION

Rapid and efficient mixing is essential in several applications of microfluidic systems such as biomedical and chemical diagnosis, process engineering and environmental monitoring. Due to the small transverse dimensions of the microchannels, the Reynolds number is low and the flow is mostly laminar with small convective effect; consequently, mixing occurs predominantly by molecular diffusion which is too slow for most applications where extremely short intervals are required. Therefore, with the aim of enhancing mass transfer in microchannel devices, different designs of micromixers have been presented in the literature and can be mostly classified in two types, passive and active. Passive micromixers use diffusion and chaotic advection as main mixing mechanism, whereas active micromixers use external energy fields to generate disturbance and mixing. Nguyen and Wu (2005) and Hessel *et al* (2005) have presented comprehensive reviews of existing micromixers.

Passive micromixers have been preferred in most applications due to their simple design, easiness of fabrication and integration compared to active ones. The classical T and Y shape designs have been tested numerically and experimentally (Gobby *et al* 2001, Engler *et al* 2004, Wong *et al* 2004) to show good mixing for Re as high as 200 but being ineffective at lower values, and different modifications in design have been introduced with the aim of increasing the effect of advection in mixing, including obstacles within the channel (Wang *et al* 2002), complex channel arrangement such as three dimensional serpentine design of outlet channel (Liu *et al* 2000), wall channel structures such as ridges and grooves (Johnson *et al* 2002, Stroock *et al* 2002). Other passive designs that increase the interfacial surface of the two streams are the serial multilayer structures for lamination of two liquid streams

*Author of correspondence

(Branebjerg *et al* 1996) and micronozzles for injection of one fluid into the other (Miyakel *et al* 1993).

Nevertheless, the above designs give more complexity to fabrication. To have simple designs, a solution could be to use the flow instabilities and patterns generated in the initial mixing region of the device and to optimize then the flow conditions and some geometry features to achieve more efficient mixing. Few studies have been made with this approach to design; Gobby *et al* (2001) evaluated numerically the T-type microfluidic mixer in 2-D to identify the mixing characteristics for gas flow and the effect of fluid speed and design parameters on mixing length, Wong *et al* (2004) used experiments and numerical simulations in micro T-mixers to determine the effect on mixing of asymmetrical flow conditions at the inlets and the generation of vortices and secondary flows at the junction, Bothe *et al* (2006) evaluated the mixing characteristics of a T-shaped micromixer for three different flow regimes to conclude that only the called engulfment flow with intertwinement of the input streams leads to efficient mixing by rolling up the initial planar contact area, Kockmann *et al* (2006a, 2006b) presented the design, fabrication and mixing characteristics of different mixer configurations, three variations of the T-mixer and one tangential mixer, that give a high throughput of aqueous solutions with mixing enhanced by vortical structures formed inside the micromixers, Yang *et al* (2006) proposed a passive micromixer in which mixing is enhanced by large 3-D flow vortex generated in a chamber where two counterflow fluids are self-driven by surface tension.

In the present study, we analyze a new configuration of the T-shaped micromixer. The basic T-type micromixer geometry is varied systematically to become a 3-D T-shaped micromixer where the two inlet channels and the straight mixing channel are connected in a T-junction zone defined by the difference in levels of the top wall of the top inlet channel and the bottom wall of the bottom inlet channel, the width of the mixing channel and the angles formed by the inlet channels and the mixing channel. Under the operation conditions and geometric dimensions implemented in this study, the designs show fluid from one side swapping to the other side and both fluids forming a circular vortex in the mixing channel which is elongated to form a sort of helical flow pattern. The interface between the two fluids rolls up within the formed vortex to enhance dramatically the mixing quality.

A systematic methodology that combines CFD analyses with numerical optimization is employed to evaluate mixing quality and pressure loss in different configurations adopted by the 3-D T-mixer and to identify the optimum ones, which show maximum mixing quality (mixing index) with minimum pressure loss.

2 METHODOLOGY

The basic 3D T-shaped micromixer and the geometric dimensions used for parameterization and analysis are shown in figure 1. Since only the cross-section dimensions of the mixing channel and the angles formed by the inlet channels are variable, the microstructured device does not include a mixing chamber and has simple inlet, contact and mixing zones in straight channels. Therefore the fabrication involves basically the formation of microchannels in material substrates.

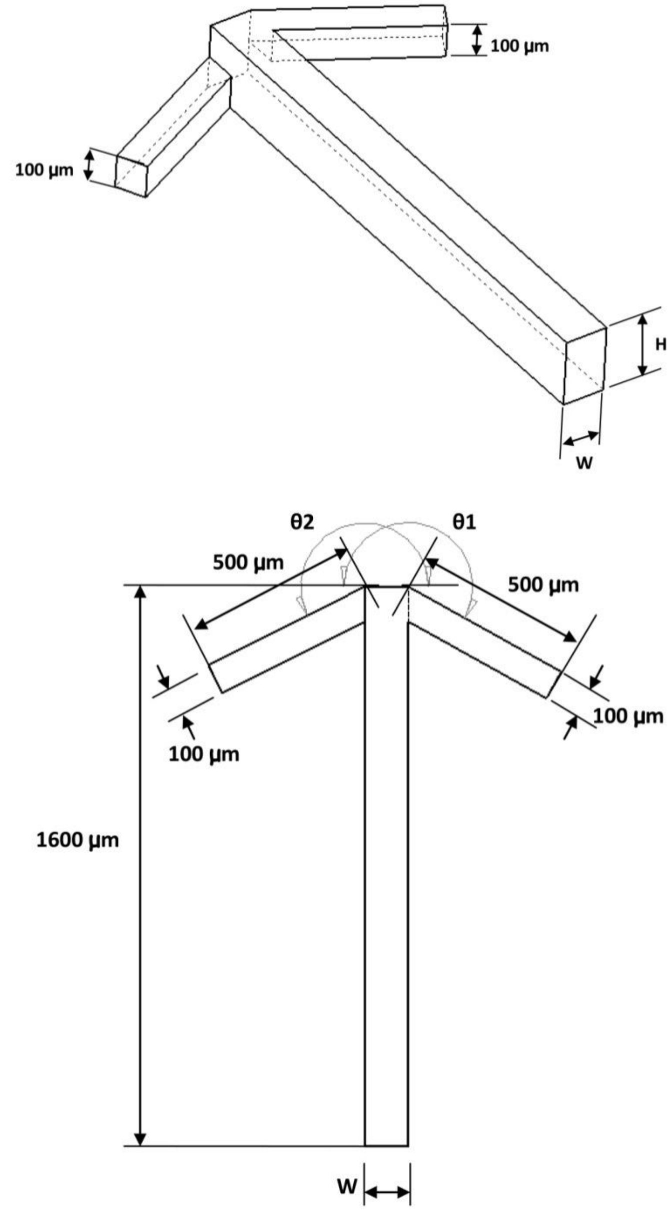

Fig. 1 Isometric view (above) and top view of the 3-D T mixer showing dimensions and geometric parameters.

For the design and optimization of the micromixer, a systematic procedure presented by Cortes-Quiroz *et al* (2008) is employed. It combines Computational Fluid Dynamics (CFD) with an optimization strategy based on the use of Design of Experiments (DOE), Surrogate Modeling (SM) and Multi-Objective Genetic Algorithm (MOGA). The DOE explores the space of design parameters and provides a table of sampling designs which are evaluated with CFD to obtain the corresponding performance parameters. The design and performance parameters are used by the SM technique to create the approximate correlate functions (response surfaces). Finally, the MOGA is run on the response surfaces to determine the Pareto front (Pf) of optimum designs, where the best compromise of the performance parameters (mixing index and pressure loss) can be chosen to fulfill the design specifications. CFD simulations are carried out to evaluate the accuracy of the predicted performance parameters.

In this study, the models are defined on the basis of the geometric features or design parameters presented in figure 1. The ranges of the four design parameters are: H [100-225 μm], W [100-225 μm], θ1 [150-210 degrees] and θ2 [150-210 degrees]. Two DOE techniques have been used: Optimal Latin Hypercube (OLH) which uses the same number of levels for each design parameter than the number of experiments (configurations or design points) with combination optimized to evenly spread design points within *n*-dimensional space defined by *n* design parameters, *n* = 25 in this study, and the Taguchi's Orthogonal Array (OA) (Taguchi 1987) which performs a fractional factorial experiment to maintain orthogonality (independence) among the various parameters and interactions, here the OA L_{27} was used to have 3 levels for each parameter organized in 27 configurations. In these configurations, two performance parameters are evaluated by using CFD, the mixing index and the pressure loss in the mixing channel. The correlation of the design and performance parameters is obtained with the surrogate model Radial Basis Function (RBF) (Hardy 1971, 1990; Kansa 1990). Finally, the Non-dominated Sorting Genetic Algorithm (NSGA-II) (Deb *et al* 2000) is applied on the approximate response surfaces to find the optimum cases that give the trade-off of maximum mixing index and minimum pressure loss.

2.1 Numerical simulation

Numerical simulations of the transport process in the 3-D T-mixer models are performed to investigate the mixing quality achieved in the geometric configurations defined by the DOE. The CFD code used for this study is the commercial Navier-Stokes Solver CFX-11 (ANSYS Europe Ltd. 2007) which is based on the Finite Volume Method. The geometries of different configurations were constructed and meshed by using the commercial mesh generator CFX-Mesh (Ansys Europe Ltd. 2007).

The flow is defined viscous, isothermal, incompressible, laminar and in steady-state, for which continuity equation (1), momentum equation (2) and species convection-diffusion equation (3) are solved.

$$\nabla.\boldsymbol{V} = 0 \tag{1}$$

$$\rho\boldsymbol{V}.\nabla\boldsymbol{V} = -\nabla P + \mu\nabla^2\boldsymbol{V} \tag{2}$$

$$\boldsymbol{V}.\nabla c = D\nabla^2 c \tag{3}$$

where ρ and μ are the density and viscosity of the fluid respectively, $\boldsymbol{V}$ is the velocity vector, P is the pressure, c is the mass fraction or concentration of the fluid under analysis and D is the diffusion coefficient of the fluid in the other fluid. Advection terms in each equation are discretized with a second order differencing scheme which minimize numerical diffusion in the results. The simulations were defined to reach convergence when the normalized residual for the mass fraction fell below 1 x 10^{-5}.

The boundary condition of the velocity at the inlets is mass inflow so that only the component in the direction of bulk flow exists to have a uniform velocity profile and the other components are zero. The velocity values at the inlets are equal and give a laminar flow regime with Reynolds numbers approximately equal to 100 and 250 in the mixing channel, and also a fixed inlet velocity of 1.3145 m/s was used for the case at fixed flow rate in the mixing channel. Along the walls, non-slip boundary condition is used for the tangential velocity component whereas the normal component is zero. At the outlet end of the mixing channel, a constant pressure condition (gauge pressure P = 0) is specified. Water at 25ºC and ethanol are used for the study of a case at fixed flow rate in the mixing channel, for which the diffusion coefficient of ethanol in water is D_{ew} = 8.4 x 10E-10 m^2/s. Water at 25 ºC and a solution of fluorescein in water are the fluids used for the study of cases at fixed Re numbers in the mixing channel, the physical properties of the solution have been considered the same than the ones of water, the diffusion coefficient of the fluorescein solution in water is taken D_{fw} = 1.8 x 10E-09 m^2/s. The boundary conditions for the species balance are mass fractions equal to 0 at the inlet where pure water is fed and equal to 1 at the inlet where the other fluid is fed. Flow vector fields, pressure and mass fraction contours from the simulations results are examined to ensure that the boundary conditions are fulfilled.

A variable mesh composed of tetrahedral elements and prism elements (adjacent to walls) is used and arranged to provide sufficient resolution for boundary layers near the fluid-solid interface on the walls of the channels. In order to obtain mesh-independent results from the simulations, a preliminary mesh size sensitivity study was carried out to determine the interval size of convergence.

2.2 Mixing characterization

In order to measure and compare the mixing intensity using the outputs from CFD simulations one can define a mixing index based on mass concentration distribution. In this study, the definition of mixing index is based on the intensity of segregation introduced by Danckwerts (1952), and is given by

$$Mi = 1 - \sqrt{\frac{\int_A \left(c - \bar{c}\right)^2 \mathrm{d}A}{A \cdot \bar{c}\left(1 - \bar{c}\right)}} \tag{4}$$

where c is the concentration distribution at the selected cross-section plane (in this study, it is the outlet plane at the end of the mixing channel), $\bar{c}$ is the averaged value of the concentration field on the plane and A is the area of the plane. *Mi* reaches a value of 0 for a complete segregated system and a value of 1 for the homogeneously mixed case. The mass concentration information from CFD analyses is used in equation 4.

3 RESULTS AND ANALYSIS

The study cases are grouped according to the fluids in use and the flow conditions.

For the first case, the same constant velocity is defined in both inlet channels and, since the cross-section area and aspect ratio of the inlet channels are fixed, it results in the same flow rate in the mixing channel of the 27 configurations defined by the Taguchi's Orthogonal Array L_{27}. Therefore, the Re number in the mixing channel is in the order of 150. The fluids to be mixed are water and ethanol. This case is an example of optimization of the design based on a fixed flow rate, which is an operation condition that defines the amount of mixed material volume that can be formed per time. Also, the fluids properties give a variable mass flow rate.

For the second case, the Re number is fixed in the mixing channel by varying the velocities in the inlet channels, which have the same value in both inlet channels. Therefore, the optimization is based on the Re number in the mixing channel and it is applied to the mixing of aqueous dye solution (fluorescein in deionized water). For Re = 250 in the mixing channel, 25 configurations defined by the OLH technique have been evaluated numerically as the first step of the optimization procedure.

The Mixing index (equation 4) and the pressure loss are calculated from simulations and used as performance parameters for the optimization of the 3-D T-mixer. For all the configurations evaluated in the present study, the pressure loss is calculated in the last 1300 microns length of the mixing channel. By doing so, the calculation is made only in the mixing channel and with the bulk mixing fluid moving downstream.

For the case at fixed flow rate in the mixing channel (inlet velocity in the channels = 1.3145 m/s), the results from applying the optimization procedure gives the Pareto front (Pf) of the optimum configurations. Seven of the design points in the Pf were chosen and evaluated by CFD to obtain the curve in figure 2 which is shown together to the curve predicted by the MOGA in the optimization procedure. The values of the corresponding four design parameters and the output parameters from CFD are shown in table 1. Since the predicted optimum values for the performance parameters comes from the double objective of maximizing mixing and minimizing pressure loss, it can explain the displacement of the 'predicted curve" towards lower values of pressure and higher values of Mixing index compared to results given by CFD. Nevertheless, the trend of both results (curves) is quite close. More accurate response surfaces could be tried to reduce the gap between the two curves in fig. 2. In table 1 one can see that the values of H and W are getting smaller along the designs of the Pf what can explain the increment of pressure loss in the mixing channel, but the objective of having the highest mixing quality for the corresponding value of pressure loss is also reached by the configurations given finally by the angles θ1 and θ2 formed by the inlet channels. These angle values tend to be closer to 180 degrees what can be explained by the longer contact time of the fluids in the T-junction which help mixing but also promotes higher value of pressure, criteria that are optimized inversely. The evolution of the mass fraction distribution on cross sections along the mixing channel of the 3-D T-mixer configurations of the Pf can be seen in figure 1A.

Before applying the optimization on the case at fixed Re in the mixing channel, a parametric study has been made by preparing several models of the 3-D T-mixer with θ1 and θ2 kept constant at 180 degrees. For this study, only the cross-section of the mixing channel is changed, i.e., the aspect ratio is

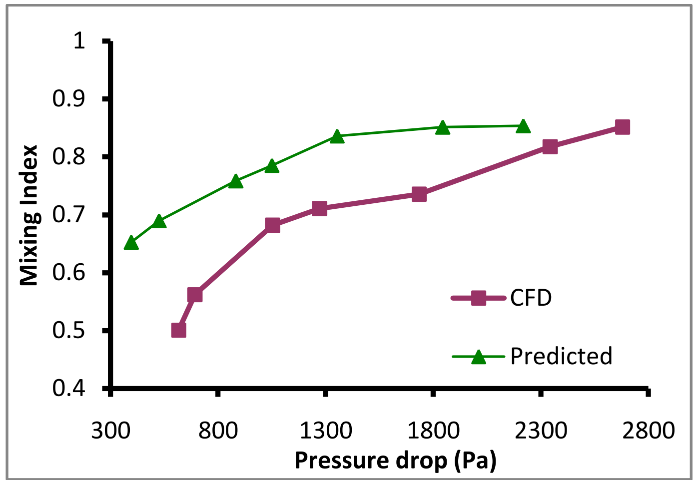

Fig. 2 Mixing index vs. pressure loss in seven selected designs of the Pareto front from multi-objective optimization. Case: Water-Ethanol, fixed flow rate in mixing channel.

Table 1 Geometric dimensions and performance outputs from CFD for the Pf designs of 3-D T-mixer with fixed flow rate.

H (µm)	W (µm)	θ1	θ2	ΔP (Pa)	Mixing Index
224.93	225.00	150.02	210.00	615.74	0.5011
224.91	224.97	150.28	202.64	692.63	0.5623
225.00	197.02	159.93	190.85	1053.1	0.6816
224.67	178.67	174.34	191.30	1271.9	0.7104
207.39	162.79	187.55	188.34	1733.5	0.7356
193.89	149.43	191.51	189.13	2344.3	0.8180
187.52	143.26	191.77	188.41	2678.9	0.8514

variable and, so, the position of one inlet channel with respect to the other also changes. A first series of designs is developed for a fixed width, W = 100 mm, but a variable height H that goes from 100 (Aspect ratio, AR = 1.0) to 200 (AR = 2.0) and numerically solved for different Re in 50-700. The results are shown in fig. 3. The second series corresponds to designs with a fixed height, H = 200 mm, but a variable height W that goes down from 200 (Aspect ratio, AR = 1.0) to 125 (AR = 1.60); the CFD analysis on these designs, for Re in 50-700, is depicted in fig. 4 that shows the results of Mixing index vs. Re. Figs. 3 and 4 also show the results from a typical T-mixer with mixing channel width, W = 200, and height, H = 100 (AR = 0.5).

From figures 3 and 4, one can observe that for almost all the operation conditions (Re) the mixing efficiency of any 3-D T-mixer design is much higher than of a standard T-mixer (AR = 0.5). The curve of the simple T-mixer is in agreement with previous work (Dreher *et al* 2009) that identifies mixing quality enhancement from Re ~ 140 and a pulsating flow at Re > 240.

It is important to say that most of the 3-D T-mixer designs come into unsteady regimen at Re >=500 and they need more evaluation for their full flow characterization; only designs with fixed W stays in steady state even at Re = 700 with the exemption of the design with AR = 1.25 which also becomes unsteady at Re = 500.

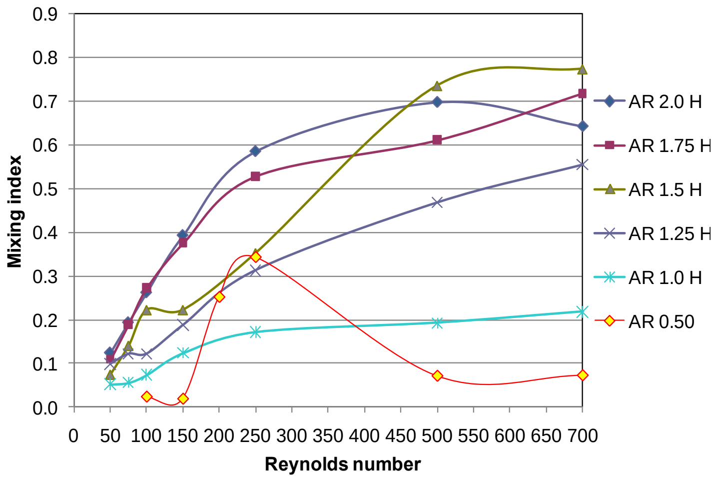

Fig. 3 Mixing index vs. Re for fixed W = 100 and variable H.

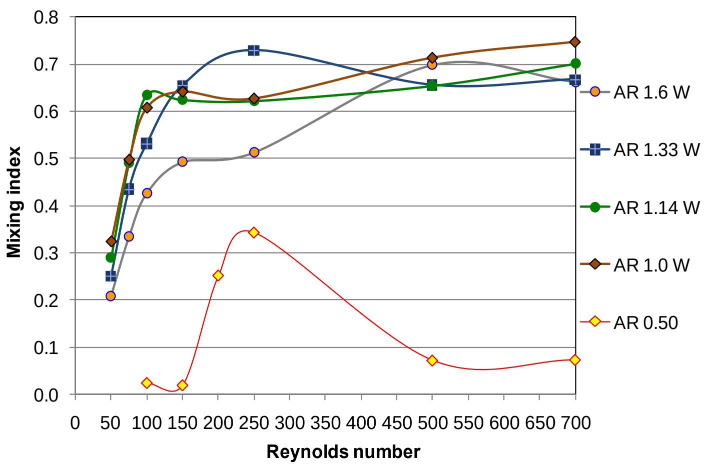

Fig. 4 Mixing index vs. Re for fixed H = 200 and variable W.

In figures 3 and 4, the values of mixing index in the designs that show unsteady regimen are the values obtained at the outlet of the mixing channel, after double the time the flow reaches this end. Comparing figures 3 and 4, one can see the designs with fixed H = 200 and variable W in 125-200 µm are giving high level of mixing index even for Re in 150-500. For Re = 250, design with AR = 1.33 gives Mi > 0.7.

For the optimization at a fixed Re in the mixing channel, the results at Re = 250 from the optimization procedure and CFD analysis are compared in fig. 5 for seven selected configurations from the Pareto front. The values from CFD of the corresponding four design parameters and the output parameters are shown in table 2. Some designs at the left end of the 'predicted curve" show the same position in the graph as it happens in fig.2, i.e. they give lower values of pressure and higher values of Mixing index compared to results given by CFD, but designs towards the right end of this curve shows slightly higher values of pressure loss. Nevertheless, the trend of predicted and CFD results is similar. In table 3 one can see that the values of H and W are getting smaller along the designs of the Pf what can explain the increment of pressure loss in the mixing channel, but the objective of having the highest mixing quality for the corresponding value of pressure loss is also reached by the configurations given finally by the angles θ1 and θ2 formed by the inlet channels. But in this case the angle values do not tend to be closer to 180 but to 210 degrees, what could have an explanation on the higher Re number used in these configurations; both values of θ1 and θ2 close to the highest value in their range, 210 degrees, would also give longer contact of the fluids in the T-junction which helps mixing.

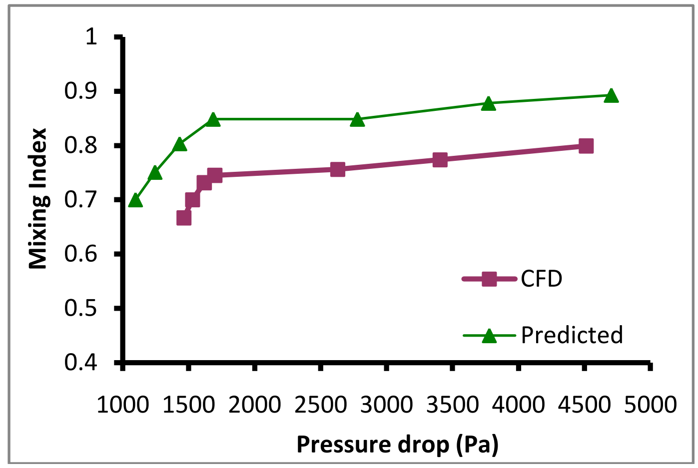

Fig. 5 Mixing Index vs. Pressure loss in selected designs of the Pareto front from multi-objective optimization. Case: Water-Fluorescein solution in DI water, Re = 250 in mixing channel.

Table 2 Geometric dimensions and performance outputs from CFD for the Pf designs of 3-D T-mixer with Re = 250.

H (µm)	W (µm)	θ1	θ2	V_{in} (m/s)	ΔP (Pa)	Mi
225.00	225.00	151.72	210.00	2.5104	1463.2	0.666
224.92	225.00	174.72	205.64	2.5099	1529.1	0.700
225.00	225.00	206.42	210.00	2.5104	1619.5	0.731
222.00	225.00	210.00	165.08	2.4936	1699.1	0.745
178.36	188.25	210.00	198.27	2.0452	2629	0.756
162.18	164.23	209.94	208.34	1.8210	3404.9	0.774
149.46	147.82	210.00	203.47	1.6584	4511.9	0.799

Figure 1A shows the contours of mass fraction distribution of water on 16 cross sections of the mixing channel of the optimum 3-D T-mixer design defined in fig. 2 and table 1. Similar contours of mass fraction result from the optimum design of fig. 5 and table 2. In fig. 1A, the length in microns given for each cross section corresponds to the distance measured from the rear wall of the mixing channel. The letters (a) to (g) in the figure correspond to the 3-D T-mixer configurations of table 2 and they go from the design with lowest mixing index and pressure loss to the one with the highest mixing index and pressure loss, according to the curves in fig. 2. These contours and the fluids streamlines shown for one of the configurations demonstrate that for the efficient designs the mixing is highly enhanced by the vortex formed in the mixing channel which starts in the meeting zone of the two fluids.

4 EXPERIMENTAL WORK

The first experiments on the presented 3-D T-mixer have been made on the original manufactured model which has the following dimensions: H = 200 μm, W = 100 μm, θ1= θ2 = 180 degrees, and inlet channels with cross section 100 x 100 μm. The device was fabricated in polymethylmethacrylate (PMMA) by Computer Numerical Control (CNC) micromachining technique. An epifluorescent microscope is used to visualize the streams of de-ionized water and aqueous solution of Fluorescein that is used as fluorescent dye. A high resolution CCD camera is utilized for taking pictures with a 10x magnification. Different Re numbers are applied for the flow in the mixing channel with symmetrical entry conditions. Figure 6 shows the state of mixing at Re = 150, with a vortex-flow clearly formed in the mixing channel; due to the configuration of the contacting zone in the 3-D T-mixer, the DI-water (black in the figure) reaches the other side of the mixing channel as well as Fluorescein solution (green in the figure) does to continue both mixing in a rolling vortex flow.

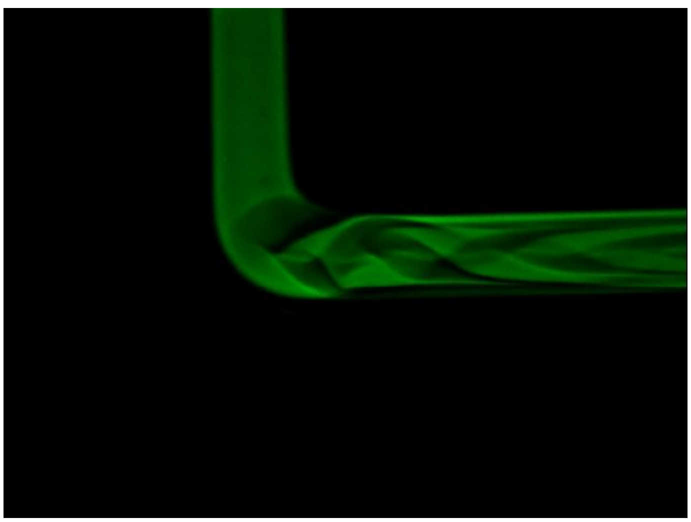

Fig. 6 Microcopy image (focus plane at 120 μm from the bottom of the mixing channel) of flow in 3-D T-mixer, Re = 150, symmetrical flow conditions at inlets.

In this case, the flow conditions are nearly stationary and the flow structures stay almost the same which make possible to examine different levels along the mixing channel depth with confocal or deconvolution microscopy. This work is in process and the purpose is to evaluate the presence of different flow regimes under different flow conditions, especially in the configurations that result from the optimization procedure.

5 CONCLUSIONS

A systematic evaluation of flow characteristics and mixing performances has been made on a proposed 3-D T-shaped micromixer. The geometries defined by four geometric parameters allow the designs to give to the flow different characteristics in the T-junction and consequently in the mixing channel that result in enhanced mixing levels with controlled pressure loss. This control is possible with the use of a systematic design and optimization methodology based on CFD and a numerical optimization procedure. The results show that it is possible to predict the trend of the two performance parameters for different configurations of the 3-D T-mixer that give high degree of mixing with the lower possible pressure loss. The 3-D T-mixer configuration for the mixing of two fluids has been established as a simple contact element, which shows the benefits of the resulting convective flow on mixing performance.

ACKNOWLEDGMENTS

We gratefully acknowledge the Dorothy Hodgkin Postgraduate Award (DHPA) of the Engineering and Physical Sciences Research Council (EPSRC) of United Kingdom and Ebara Research Co. Ltd. of Japan for their financial support.

REFERENCES

ANSYS Europe Ltd. (2007). CFX 11.0 User Manual.

Bothe D., Stemich C. & Warnecke H-J. (2006). Fluid mixing in a T-shaped micro-mixer. *Chem. Eng. Sci.* **61**: 2950-2958.

Branebjerg J., Gravesen P., Krog J. P. & Nielsen C. R. (1996). Fast mixing by lamination. *Proc. IEEE MEMS 1996*, pp. 441-446.

Cortes-Quiroz C. A., Zangeneh M. & Goto A. (2009). On multi-objective optimization of geometry of staggered herringbone micromixer. *Microfluid. Nanofluid.* 7(1): 29-43.

Danckwerts P. V. (1952). The definition and measurement of some characteristics of mixtures, *Appl. Sci. Res.* **A 3**: 279-296.

Deb K., Agrawal A., Pratap T. and Meyarivan T. (2000). A fast and elitist multi-objective genetic algorithm for multi-objective optimization: NSGA-II. *Proceedings of the Parallel Problem Solving from Nature VI Conference*, pp. 849-858, Paris, France, 2000.

Dreher S., Kockmann N. & Woias P. (2009). Characterization of laminar transient flow regimes and mixing in T-shaped micromixers. Heat Transfer Engineering **30 (**1-2**)**, 91–100.

Engler M., Kockmann N., Kiefer T. & Woias P. (2004). Numerical and experimental investigations on liquid mixing in micromixers. *Chem. Eng. J.* **101**:315–322

Gobby D., Angeli P. & Gavriilidis A. (2001). Mixing characteristic of T-type microfluidic mixers. *J. Micromech. Microeng* **11**: 126–132.

Hardy, R.L. (1971). Multiquadric equations of topography and other irregular surfaces. *J Geophysical Research* **76** (8), 1905-1915.

Hardy, R.L. (1990). Theory and applications of the multiquadric-biharmonic method: 20 years of discovery, 1968-1988. *Computers and Mathematics with Applications* **19** (8-9), 163-208.

Hessel V., Lowe H. & Schonfeld F. (2005). Micromixers, a review on passive and active mixing principles. *Chem. Eng. Sci.* **60**: 2479-2501.

Johnson T. J., Ross D. & Locascio L. E. (2002). Rapid microfluidic mixing. *Anal. Chem.* **74**:45-51.

Kansa E. J. (1990). Multiquadrics- A scattered data approximation scheme with applications to computational fluid-dynamics: I. Surface approximations and partial derivative estimates. *Computers and Mathematics with Applications* **19** (8-9), pp. 127-145.

Kockmann N., Kiefer T., Engler M. & Woias P. (2006). Silicon microstructures for high throughput mixing devices. *Microfluid. Nanofluid.* **2**: 327-335.

Kockmann N., Kiefer T., Engler M. & Woias P. (2006). Convective mixing and chemical reactions in microchannels with high flow rates. *Sensors and Actuators B Chem.* **117**: 495-508.

Liu R. H., Stremler M. A., Sharp K. V., Olsen M. G., Santiago J. G., Adrian R. J., Aref H. & Beebe D. J. (2000). Passive mixing in a three-dimensional serpentine microchannel. *J. Microelectromech. Syst.* **9**: 190-197.

Miyakel R, Lammerinkz T. S. J., Elwenspoek M. & Fluitman J. H. J. (1993). Micro mixer with fast diffusion. *Proc. IEEE MEMS 1993*, pp. 248-253.

Nguyen N. and Wu Z. (2005). Micromixers-a review. *Journal of Micromechanics and Microengineering* **15**: R1-R16.

Stroock A. D., Dertinger S. K. W., Ajdari A., Mezic I., Stone H. A. & Whitesides G. M. (2002). Chaotic mixer for microchannels. *Science* **295**: 647–651.

Taguchi G. (1987). Systems of Experimental Design, Vols. 1 and 2. New York: Kraus International.

Wong S. H., Michael C. L. Ward & Wharton C. W. (2004) Micro T-mixer as a rapid mixing micromixer. *Sensors and Actuators B Chem.* **100**: 359-379.

Wang H., Iovenitti P., Harvey E. & Masood S. (2002). Optimizing layout of obstacles for enhanced mixing in microchannels. *Smart Mater. Structure* **11**: 662-667.

Yang I-Da, Cheng Y-F., Tseng F-G., Hsu H-T. & Chieng C-C. (2006). Surface tension driven and 3-D vortex enhanced rapid mixing microchamber. *J. Microelectromech. Syst.* ***15*** (3), 659-670.

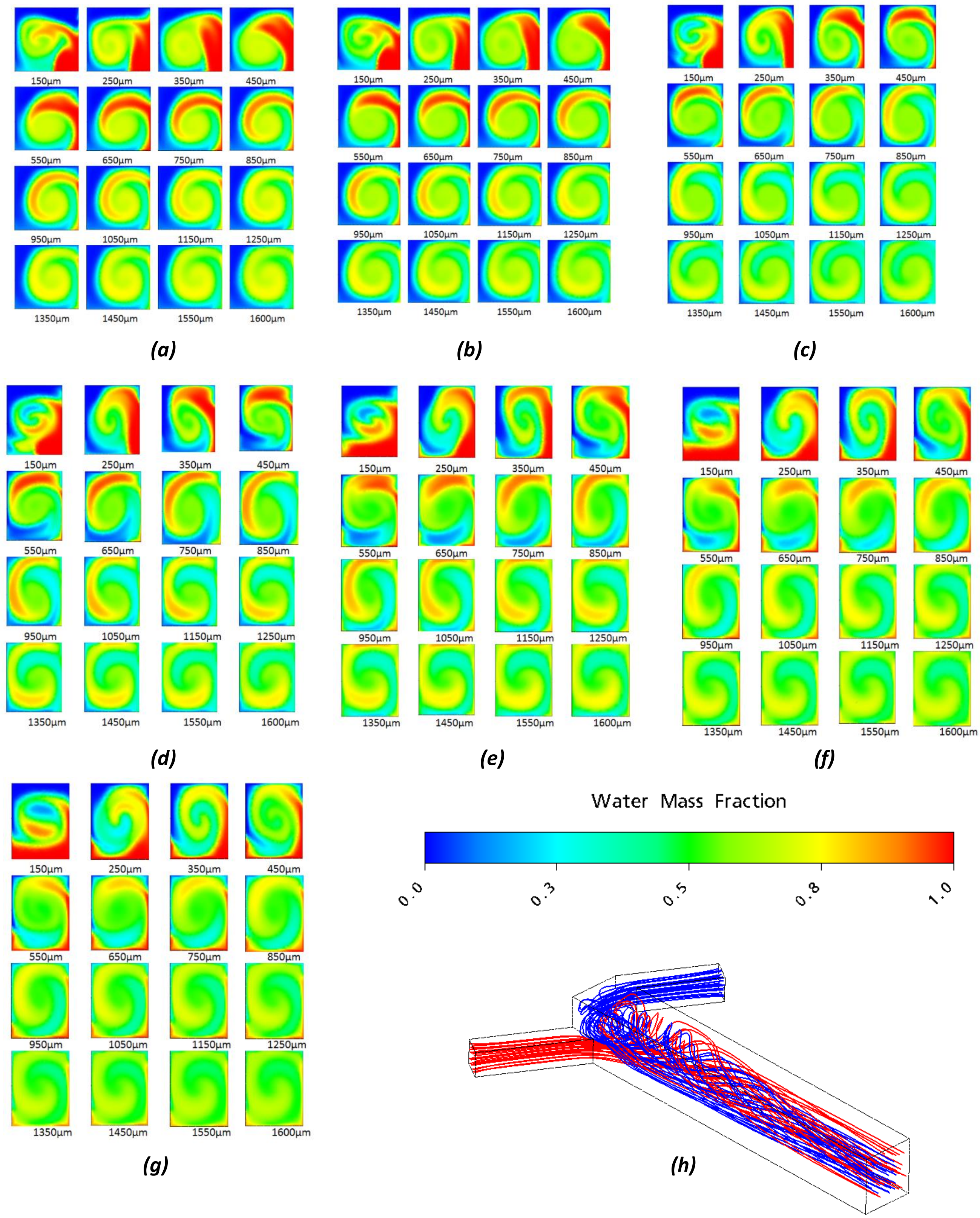

Fig. 1A (a)-(g): Mass fraction distribution contours of water on 16 cross sections of the mixing channel of the optimum 3-D T-mixer configurations defined in table 1; **(h):** Streamlines of water and ethanol in the first configuration of table 1, fluids come into the device at 1,31454 m/s.